[CANCER RESEARCH 59, 4136–4141, August 15, 1999]

Available Volume Fraction of Macromolecules in the Extravascular Space of a Fibrosarcoma: Implications for Drug Delivery[1]

Ava Krol, Julie Maresca, Mark W. Dewhirst, and Fan Yuan[2]

Departments of Biomedical Engineering [A. K., J. M., F. Y.] and Radiation Oncology [M. W. D.], Duke University, Durham, North Carolina 27708

ABSTRACT

Steric exclusion of molecules in the extravascular space of tissues can be quantified by the available volume fraction (K_{AV}). Despite its clinical importance, however, there is a paucity of data in the literature regarding the available volume fraction of macromolecules in the extravascular space of tumor tissues. In this study, we quantified K_{AV} of inulin, BSA, and dextran molecules of M_r 10,000–2,000,000 in polymer gels and fibrosarcoma tissues. The measurement involved: (*a*) sectioning of gels or tumor tissues into thin slices (~600 μm) using a Vibratome, (*b*) *ex vivo* incubation of the slices in solutions containing fluorescently labeled tracers, and (*c*) quantification of the equilibrium tracer concentrations in both slices and solutions. We found that K_{AV} in gels decreased monotonically when the M_r of dextran was increased from M_r 10,000 to 2,000,000. However, K_{AV} in tumor tissues was insensitive to the molecular weight of dextran in the range between M_r 10,000 and 40,000. There was a sharp decrease in K_{AV} from 0.28 ± 0.14 to 0.10 ± 0.06 when the molecular weight was increased from M_r 40,000 to 70,000. In addition to the molecular weight dependence, K_{AV} was heterogeneous in tumors, with intertumoral difference being greater than intratumoral variation. The interstitial fluid space, which was quantified by K_{AV} of inulin, was 50% of the total tissue volume. These data indicate that the fraction of the extravascular volume in tumors that is accessible to large therapeutic agents is heterogeneous and depends on the size of agents.

INTRODUCTION

Interstitial structure is one of the major barriers to drug delivery in solid tumors (1). Drug delivery in the interstitial space is governed by various transport parameters, including the available volume fraction (K_{AV}). K_{AV} is defined as the volume fraction in the extravascular space of tissues that is accessible to therapeutic agents (2, 3). K_{AV} depends on physicochemical properties of agents (*e.g.*, size and configuration) and volume fraction of cells as well as structure and composition of extracellular matrix (2, 4–10). An increase in K_{AV} would improve both local distribution and total accumulation of drugs in solid tumors. One strategy to increase K_{AV} is to digest extracellular matrix in tumors (7, 11). For instance, it has been shown that treatment of solid tumors with hyaluronidase improves drug accumulation in tumor tissues (12, 13).

Most K_{AV} data in the literature are from normal tissues (2, 7–9, 14–22). A few K_{AV} data from tumors are available (23–27), and most of them are associated with small molecules (*e.g.*, Na^+, Cl^-, mannitol, and EDTA; Refs. 23–26). Therefore. the available volume fraction of macromolecules has been assumed to be unity in previous numerical simulations of drug delivery in solid tumors (28–30). In this study, we developed an *ex vivo* assay for measuring K_{AV} of different macromolecules. Our results demonstrate that only a small fraction of the extravascular space in tumors is accessible to exogenous macromolecules. Therefore, the assumption of unity for K_{AV} may overestimate the total accumulation of macromolecular drugs in tumors.

MATERIALS AND METHODS

Tumor and Tracers

A rat fibrosarcoma (MCA-R) was used in the study. Tumor chunks (~1 mm in diameter) were transplanted s.c. into the right hind limb of 2-month-old female Fisher rats (weighing ~150 g; Ref. 31). When tumors reached 2 cm in diameter, rats were anesthetized with i.p. injection of pentobarbitol (50 mg/kg body weight), and tumor tissues were removed and put immediately into a centrifuge tube on ice, which contained DMEM. Then a piece of tumor tissue was glued onto a specimen block and transferred to the stage of a Vibratome (model 3000; Technical Products International, St. Louis, MO) maintained at 4°C. The tissues were then sectioned into thin slices (600 μm thick), unless otherwise specified.

Tracers used in the study included various dextran molecules of M_r 10,000–2,000,000, BSA, and inulin (Sigma Chemical Co., St. Louis, MO). Dextrans and BSA were labeled with rhodamine, and inulin was labeled with FITC. The tracers were dissolved in PBS at concentrations of 0.1–1.0 mg/ml (pH 7).

Preparation of Gels

A polymer gel was prepared to mimic connective tissues. The preparation involved dissolving gelatin (2%) and chondroitin sulfate (1%) from bovine trachea powders in PBS containing 1% BSA. The gel was formed when the polymer solution was placed in the refrigerator. A piece of gel was glued onto a specimen block and sectioned at 4°C as described above. The thickness of the gel slices was 600 μm, unless otherwise specified.

Incubation Chamber

A polycarbonate chamber was constructed to study the effect of tissue swelling on the available volume fraction. The chamber was 800 μm thick and 4 mm in diameter. Both ends of the chamber were covered with polyethylene frits. Therefore, tracers could easily diffuse into the chamber, but the volume of the chamber was fixed. Tumor tissues were sectioned into 400-μm slices and cut into discs of 4-mm diameter. The discs were sandwiched between two nylon meshes (thickness, 200 μm; and diameter, 4 mm) and placed into the chamber. Therefore, the total volume of the disc plus nylon meshes was equal to the volume of the chamber. The whole chamber was then incubated in tracer solutions.

Equilibrium Time Constant

The quantification of K_{AV} involved incubation of tissue slices in solutions of fluorescently labeled tracers and measurement of equilibrium concentrations of tracers in tissues (C_t) and solutions (C_{sol}), respectively. The time constant for reaching the concentration equilibrium was estimated by $2h^2/D$, where h is the slice thickness and D is the diffusion coefficient of tracers in tissues (obtained from Refs. 32 and 33). The prediction of the equilibrium time constant was consistent with experimental observations when the fluorescence intensity in tissues was quantified as a function of incubation time (data not shown). The same equation was also used to estimate the equilibrium time constant in the incubation of gels.

Calibration of the Concentration Measurement

Fluorescence intensities in tissues (I_t) and solutions (I_{sol}) were quantified after the equilibrium of incubation was reached. We found that both I_t and I_{sol} were linear functions of tracer concentration in solutions (C_{sol}; $r^2 > 0.9$, where r was the correlation coefficient). Furthermore, tracer concentration in tissues

Received 2/15/99; accepted 6/15/99.

The costs of publication of this article were defrayed in part by the payment of page charges. This article must therefore be hereby marked *advertisement* in accordance with 18 U.S.C. Section 1734 solely to indicate this fact.

[1] Supported in part by Whitaker Foundation Grant 97-0062 and NIH Grant P50-CA68438-02.

[2] To whom requests for reprints should be addressed, at Department of Biomedical Engineering, Box 90281, Duke University, Durham, NC 27708. Phone: (919) 660-5411; Fax: (919) 684-4488; E-mail: fyuan@acpub.duke.edu.

(C_t) was proportional to C_{sol} at the equilibrium of incubation. Therefore, $\Delta I_t = (I_t - I_{bt}) = B_t C_t$ and $\Delta I_{sol} = (I_{sol} - I_{bs}) = B_{sol} C_{sol}$, where I_{bt} and I_{bs} are the background fluorescence intensities in tissues and solutions, respectively. We found that B_{sol} was a linear function of the solution thickness (h_{sol}) in the range between 0 and 1000 μm ($r^2 > 0.9$), *i.e.*, $B_{sol} = k_{sol} h_{sol}$, where k_{sol} is a constant. However, the dependence of B_t on tissue thickness (h_t) was nonlinear, due to light scattering and absorption, which, in turn, depended on the wavelength of light, the effective penetration depth of light, the diffuse reflectance in tissues, and the intensity of the incident light (34). We found that B_t increased as a function of h_t, if h_t was <200 μm, and was nearly independent of the thickness, if h_t was >400 μm (data not shown).

A similar procedure was performed for gels, and we found that $\Delta I_{gel} = (I_{gel} - I_{bg}) = k_{gel} h_{gel} C_{gel}$, where I_{gel} and I_{bg} are fluorescence intensity of tracers and background intensity, respectively; h_{gel} is the thickness of gels; C_{gel} is the tracer concentration in gels; and k_{gel} is a constant. In solutions and gels, light scattering and adsorption could be neglected in our study because the fluorescence intensity was a linear function of both concentration and thickness. Therefore, k_{sol} and k_{gel} were determined mainly by the physicochemical properties of tracers. We found that $k_{sol} \approx k_{gel}$ and assumed that $k_{sol} = k_{gel}$ in the calculation of K_{AV}. The same assumption has been made in previous studies (6, 10).

Quantification of K_{AV}

Tumor (or gel) slices were incubated in solutions of tracers in microcentrifuge tubes at 4°C for a time period longer than $2h^2/D$. During the incubation, the solutions were stirred by a shaker (Labquake; Barnstead/Thermolyne, Dubuque, IA). At the end of incubation, K_{AV} was determined as the concentration ratio between tissues (or gels) and solutions (C_t/C_{sol} or C_{gel}/C_{sol}). The procedures for the quantification of C_t/C_{sol} and C_{gel}/C_{sol} are as follows.

Quantification of K_{AV} in Gels. After incubation of gel slices in a tracer solution, the slices were cut into 4-mm diameter discs, using a skin biopsy puncher, and transferred into plastic wells (0.6 mm in depth), which were glued on a glass microslide and filled with PBS. The wells were sealed with glass coverslips. The incubation solutions were transferred into separate wells with the same thickness. The fluorescence intensities in gel discs and the solutions were quantified via a fluorescence microscope (Axiovert 100; Zeiss, Thornwood, NY) equipped with the fluorescence filter sets for rhodamine and FITC (Omega Optical Inc., Brattleboro, VT) and a photomultiplier (model 9658B; Thorn EMI Electron Tubes, Rockaway, NJ). On the basis of the concentration calibration described above, the available volume fraction was calculated as follows:

$$K_{AV} = \frac{\Delta I_{gel}}{\Delta I_{sol}} \quad \text{(A)}$$

The quantification was performed within 2 min to minimize the amount of tracer release from gels.

Quantification of K_{AV} in Tissues. Similar to the quantification of K_{AV} in gels described above, tissue slices were incubated, cut, and transferred into the plastic wells containing PBS, and the fluorescence intensities in tissue discs and incubation solutions were quantified via the same fluorescence microscope workstation as in gel experiments. On the basis of the concentration calibration described above, K_{AV} in tumor tissues was calculated as follows:

$$K_{AV} = \alpha h_{sol} \frac{\Delta I_t}{\Delta I_{sol}} \quad \text{(B)}$$

where $\alpha = k_{sol}/B_t$, which depended only on optical properties of tissues and the wavelength of the light. It was independent of tracers and the thickness of tissue slices, if h_t was >400 μm.

To determine the value of α, we performed a separate experiment. Circular discs of tumor tissues were incubated in the solution of rhodamine-labeled dextran 10 or FITC-labeled inulin in centrifuge tubes. The number of discs (n) was 8, and the volume of the solution (V) was 200 μl. The size of discs was 7 mm in diameter (d) and 0.6 mm in thickness (h). The incubation solutions were sampled using 100-μm glass capillaries, both before (ΔI_0) and at the equilibrium state (ΔI_{eq}) of incubation, and the fluorescence intensities in capillaries were quantified using the fluorescence microscope workstation. On the basis of the mass balance of tracers in microcentrifuge tubes, K_{AV} could be determined as:

$$K_{AV} = \frac{4V}{\pi d^2 h n} \left(\frac{\Delta I_{eq}}{\Delta I_0} - 1 \right) \quad \text{(C)}$$

At the end of incubation, three tissue discs and the solution were transferred into six different plastic wells, as described above, and the mean values of fluorescence intensities in three discs $[(\Delta I_t)_{mean}]$ and solutions in three wells $[(\Delta I_{sol})_{mean}]$ were quantified. Substituting $(\Delta I_t)_{mean}$, $(\Delta I_{sol})_{mean}$, and K_{AV} obtained from Eq. C into Eq. B, α could be determined. We found that $\alpha = 1.10 \pm 0.45$ mm^{-1} (mean $\pm$ SD, $n = 4$) for rhodamine-labeled dextran 10 and $\alpha = 3.02 \pm 1.34$ mm^{-1} (mean $\pm$ SD, $n = 4$) for FITC-labeled inulin, where n is the number of tumors.

Although both Eqs. B and C can be used to determine K_{AV}, a major disadvantage of the second method is that it requires a lot of tissue from a tumor. Consequently, it cannot be used to quantify K_{AV} in small tumors and cannot reveal intratumoral variations in K_{AV}. Therefore, we used only the first method in the study, except for the determination of α.

The available volume fraction in the extravascular space of fibrosarcoma determined in this study could be larger than K_{AV} *in vivo* because tracers could enter both interstitial and vascular spaces. However, the vascular space *in vivo* occupies $<10\%$ of the total tumor volume (35, 36), and blood vessels likely collapsed after tumor removal from animals. Therefore, the overestimation of K_{AV} in this study would be significantly less than 10%.

Viability of Tumors

Viability of tumor tissues after incubation was estimated, based on the Live/Dead assay. The procedure was as follows. Tumor tissues were digested by Pronase in a solution of 900 μl of DMEM and 100 μl of Pronase (2%), for 1 h at 37°C. At the end of incubation, Pronase was removed through washing tissues in 1.5 ml of DMEM three times. Then, the tissue suspension was digested by collagenase in a solution of 800 μl of DMEM and 200 μl of collagenase (1%) for 4 h at 37°C. At the end of the incubation, the tissue suspension was washed twice in 10 ml of saline and stained with the Live/Dead fluorescent dyes (Molecular Probes, Eugene, OR) for 15 min. The numbers of red (dead) and green (viable) cells observed under a fluorescence microscope (Axiovert 100; Zeiss) were counted and compared.

Statistical Analysis

The Mann-Whitney U and Wilcoxon signed rank tests were used to compare the differences between unpaired and paired groups, respectively, and the Kruskal-Wallis test was used when more than two groups were compared. Tests were considered significant if Ps were <0.05.

RESULTS AND DISCUSSION

Available Volume Fraction

Molecular Weight Dependence. The available volume fraction of different tracers was quantified in tumor tissues (Fig. 1). We found that K_{AV} was not reduced as the molecular weight of dextran molecules increased from 10,000 to 40,000, but it decreased significantly if the M_r was $>40{,}000$ ($P < 0.01$; Fig. 1). The mechanisms of these results were not clear, but they were unlikely to be caused by polydispersity of dextran molecules. The reason is twofold. (*a*) Similar results have been observed in the study of microvascular permeability of proteins and polypeptides in tumors (37). These molecules were monodispersed, as demonstrated by SDS-PAGE analysis, but the permeability is independent of M_r in the range between 25,000 and 45,000 and decreases significantly when M_r is increased from 45,000 to 66,000 (37). (*b*) We quantified the available volume fraction in a polymer gel, using the same dextran molecules. We found that K_{AV} decreased monotonically as the size of dextran molecules increased (Fig. 1). Therefore, mechanisms related to structures of extracellular matrix need to be investigated.

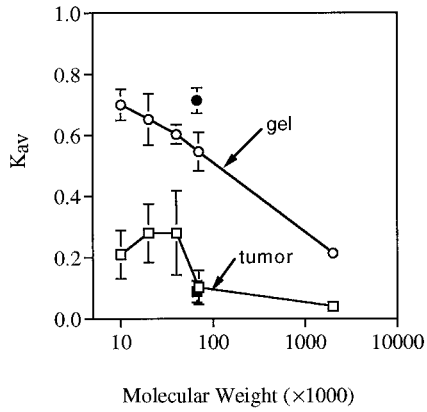

Fig. 1. The available volume fraction of dextrans (□ and ○) and BSA (■ and ●) in fibrosarcomas (□ and ■) and polymer gels (○ and ●). *Data points*, means of 24–35 measurements in six to eight fibrosarcomas (*tumor*) or means of 12 measurements in four different gel preparations (*gel*); *bars*, SD.

Structures of extracellular matrix have been studied in the bone and normal microvessels (38–42). These studies have demonstrated that the structure of extracellular matrix on endothelial cells (*i.e.*, the glycocalyx; Refs. 38 and 39) or in canaliculi (41) is not random. Fibers in the matrix are organized by albumin, which binds to glycosaminoglycan side chains of proteoglycans. These side chains form a regularly spaced lattice with the pore size of ~7 nm in diameter, the size of albumin (38, 41). Direct observations of proteoglycan structures by electron microscope have demonstrated that the distance between attachment sites of the side chains is tissue dependent (43, 44). It varies between 7 and 11 nm, except for that in the aorta, which is 17 nm (43, 44).

The proteoglycan structure discussed above might explain the significant decrease in the slope of K_{AV} profile as the molecular weight of tracers was increased from M_r 40,000 to 70,000 (Fig. 1) because concentrations of hyaluronic acid and chondroitin sulfate are found to be elevated in a variety of epithelial and mesenchymal tumors (45). To test this hypothesis, we prepared a polymer gel composed of 2% gelatin, 1% chondroitin sulfate, and 1% BSA and quantified K_{AV} in gels (Fig. 1). We found that there was no significant change in the slope of K_{AV} profile as the M_r of tracers was increased from 10,000 to 70,000 (Fig. 1) and that the shape of the curve shown in Fig. 1 could not be changed by increasing the concentrations of both chondroitin sulfate and BSA to 5% or by removing BSA from gels (data not shown). The lack of an abrupt change in the slope indicated that there was no cutoff pore size in gels. These results were consistent with previous studies using other polymer gels: polyacrylamide (6, 10), collagen (2), and hyaluronate (2). The discrepancy between K_{AV} in gels and K_{AV} in tumor tissues is likely related to the orientation of fibers in matrices. Mathematical models of spheres in a random suspension of fibers fit well to the K_{AV} data in polymer gels (10, 46–49). However, mathematical models of spheres in matrices with regular patterns of fiber orientation predict a cutoff pore size in gels (50). Molecules larger than the pore size will be excluded from matrices (50).

There was no significant difference in K_{AV} between dextran 70 and BSA in tumors (Fig. 1). However, K_{AV} of albumin was significantly higher than that of dextran 70 in gels ($P < 0.01$; Fig. 1). The difference between tumors and gels could be due to nonspecific binding of albumin to gelatin and chondroitin sulfate.

Comparison with Previous Studies. Few data on the available volume fraction of macromolecules in solid tumors are available in the literature. However, the available volume fraction of macromolecules has been studied extensively in normal tissues (2, 7–9, 14–22). In these studies, K_{AV} of albumin ranged from 0.04 to 0.22 (15–20, 22), except for two extreme cases: K_{AV} of albumin is <0.01 in cartilage (8) and averages 0.41 the umbilical cord (7). Therefore, the albumin results in the fibrosarcoma model (0.04–0.17) are within the range reported for normal tissues.

The molecular weight dependence of K_{AV} has also been investigated in cartilage (8, 14) and umbilical cord (7, 9) using dextrans and globular proteins. It has been found that K_{AV} decreases monotonically in both tissues as the molecular size is increased.

Interstitial Fluid Space and the Partition Coefficient. Steric molecular exclusion in the extravascular space of tissues depends on structure of extracellular matrix and volume of the interstitial fluid space. The latter has been quantified in solid tumors, using Na^+, Cl^-, mannitol, and EDTA (for review see Ref. 51). Inulin has also been used as a marker for the interstitial fluid space in normal (52) and tumor (27) tissues. These studies have demonstrated that there is no significant difference between inulin space and sodium (27) or mannitol (52) space.

The ratio of available volume fractions between tracers and interstitial fluid is defined as the partition coefficient (3). To estimate the partition coefficient of dextran 10 in the fibrosarcoma, we quantified the available volume fractions to dextran 10 and inulin, respectively, in the same tumor. We found that the available volume fraction (mean ± SD) of dextran 10 (0.26 ± 0.09, $n = 4$) was about one-half of that of inulin (0.50 ± 0.11, $n = 4$). The difference was statistically significant ($P < 0.05$). These data suggested that the partition coefficient of dextran 10 was 0.52, *i.e.*, 52% of the interstitial fluid space in the rat fibrosarcoma was available to dextran 10. The result of the available volume fraction of inulin is consistent with previous studies of fibrosarcomas (51). In these studies, the interstitial fluid space in fibrosarcomas varied between 0.33 and 0.60 (51).

Heterogeneity. The available volume fraction was heterogeneous both within a tumor and among different tumors (Fig. 2). We compared the available volume fraction of dextran 10 in different regions of a tumor and found that the coefficient of variation was between 14 and 30% (Fig. 2). However, if the mean values of the available volume fraction from each tumor were compared, the coefficient of variation was 45%. These data suggest that the difference in tissue structure is more significant between tumors than within a tumor.

The heterogeneity could be caused by variations in the volume fraction of cells and structures of extracellular matrix. For example, K_{AV} of albumin in hyaluronate gels decreases exponentially as a function of hyaluronate concentration and reaches a plateau at a concentration of 25 mg/ml, and K_{AV} decreases linearly in colla-

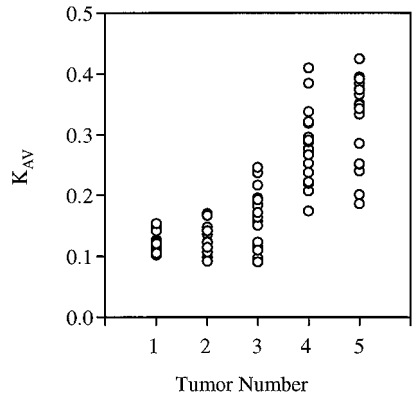

Fig. 2. The available volume fraction of dextran 10 in five different fibrosarcomas. ○, individual measurements of K_{AV}. In each tumor slice, measurements were performed at three different locations. The number of slices from one tumor varied between five and six.

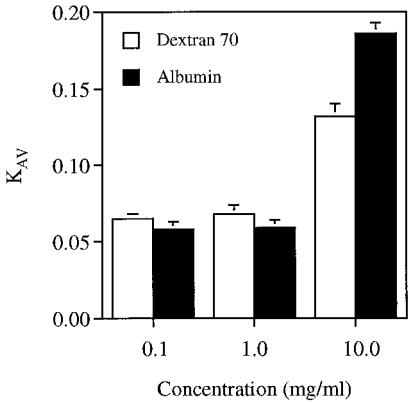

Fig. 3. Fibrosarcoma tissue slices were incubated in the solution of dextran 70 or albumin at the concentration of 0.l, 1.0, or 10 mg/ml. For both dextran 70 and albumin, there was no statistical difference in the available volume fraction between 0.1 mg/ml and 1.0 mg/ml groups ($P > 0.5$; Mann-Whitney U Test). However, the available volume fractions of both tracers were increased significantly if the concentrations of tracers were increased to 10 mg/ml. *Columns*, means; *bars*, SD.

gen gels in the range of collagen concentration between 0 and 100 mg/ml (2).

Methods of Quantification

Three different methods have been used in previous studies to measure the available volume fraction of macromolecules. One involves direct collection of the interstitial fluid and determination of its plasma protein concentration. The ratio of the concentration in the interstitial fluid *versus* that in the plasma gives the partition coefficient of plasma proteins (20, 22). The second method is similar to the first but can be used to measure K_{AV} of exogenous macromolecules. The technique involves injection of tracers into the systemic circulation of animals and measurement of equilibrium concentration ratio between tissues and the plasma (27). One question associated with this technique is how to determine the time constant of equilibrium between tissues and the plasma. The equilibrium time constant depends on rate of plasma clearance and interstitial penetration of tracers. If plasma clearance is faster than interstitial diffusion, then the equilibrium state may never be reached. Wiig *et al*. (17) circumvent this problem by maintaining the plasma concentration at a constant level. In their study, tracers are released slowly over a period of 2 weeks via an implanted osmotic pump. In doing so, they are able to establish the concentration equilibrium between the plasma and normal tissues. However, this method may not be suitable for determining K_{AV} in tumor tissues. The reason is twofold. (*a*) Extravasation in solid tumors is heterogeneous, and regions in which tumor vessels are impermeable to macromolecules exist (1, 53). The heterogeneous extravasation causes nonuniform distribution of macromolecules. (*b*) The interstitial fluid pressure is elevated in solid tumors (1). The pressure gradient may force extravasated macromolecules to move to the periphery of tumors. Therefore, the concentration of tracers may be higher in the periphery than at the center of tumors (1, 54). The third method for determining K_{AV} involves incubation of tissue slices *ex vivo* in solutions containing tracers of interest and measurement of equilibrium concentrations of tracers in both tissues and solutions (2, 7–9, 14–16, 18, 19, 21). The advantage of this method is that concentration equilibrium between tissues and solutions can be established reproducibly and the equilibrium time constant is predictable. However, several key issues regarding potential problems in the measurement still need to be addressed.

Viability of Tumor Cells. The *ex vivo* incubation of tissue slices in solutions of fluorescently labeled tracers may cause cell death. Therefore, a viability test was performed in our study. Tissue slices were incubated in PBS at 4°C for 24 h, which was longer than any incubation time in the K_{AV} study. The fraction of viable cells in tissues was quantified both before and at the end of the incubation. Immediately before the incubation, the fraction of viable cells in tissues was ~89%. After a 24-h incubation, the fraction of viable cells was ~90%. Therefore, the effect of incubation on cell viability could be neglected.

Effect of Tracer Concentration. Measurements of K_{AV} might be affected by the concentration of tracers. We found that K_{AV} of both dextran 70 and BSA at the concentration of 0.1 mg/ml were not statistically different from those at 1.0 mg/ml (Fig. 3). However, both K_{AV}s were increased significantly if the concentration was 10 mg/ml (Fig. 3). There are two possible explanations for the data in Fig. 3. The first is aggregation of tracers in tissues, although no aggregation was observed in solutions. The second is the nonlinear partitioning phenomenon (55). Both theoretical and experimental studies have demonstrated that the partitioning of molecules between porous media and exterior solutions increases with the concentration of solutions, if the concentration is higher than a threshold level (55). To avoid the concentration effect on K_{AV}, we always used a tracer concentration of $<$1.0 mg/ml in our experiments.

Effect of Tissue Swelling. One of the major concerns associated with the *ex vivo* incubation of tissues is the change in structure due to swelling (7, 11, 56). The fibrosarcoma tissue swelled in physiological saline. We found that the weight of tissue increased 2.6 $\pm$ 2.0% (mean $\pm$ SD, $n = 6$) during the first hour of incubation and that there was no significant change in the weight from 1 to 6 h ($P = 0.26$). The weight increase was 7.2 $\pm$ 3.2% (mean $\pm$ SD, $n = 6$) after 24 h of incubation.

The swelling may change the available volume fraction of macromolecules (9, 57). Therefore, minimizing tissue swelling will reduce error in measurements. In general, tissue swelling can be caused by (*a*) swelling of cells (58) and/or (*b*) swelling of extracellular matrix (7, 11, 56, 59–61). The former can be minimized using isotonic solutions, whereas the latter can be controlled using several methods. The swelling of extracellular matrix is predominantly caused by the Gibbs-Donnan osmotic pressure of proteoglycans because treatment of tissues with hyaluronidase results in de-swelling of preswelled tissues (7, 11). Swelling of extracellular matrix can be minimized by using hypertonic solutions (11, 56, 59–61) or supplementing incubation medium with polybase (*e.g.*, polylysine; Ref. 11). However, the

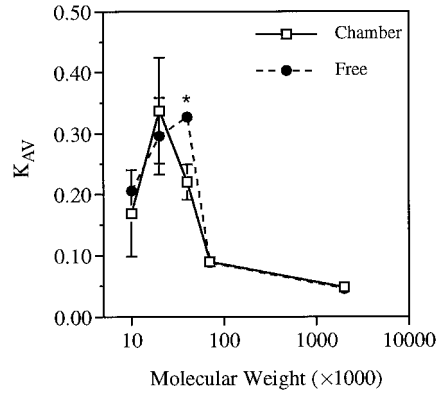

Fig. 4. Effect of tissue swelling on the available volume fraction of dextrans in fibrosarcomas. All slices were obtained from a single tumor, and these slices were incubated either in chambers (□) or freely (●) in dextran solutions. At the end of incubation, the available volume fraction was quantified in each groups. *Data points*, means of nine measurements in three slices; *bars*, SD. *, K_{AV} of dextran 40 in the free incubation group is statistically higher than that in the chamber group. There was no difference in K_{AV} of other tracers between two groups.

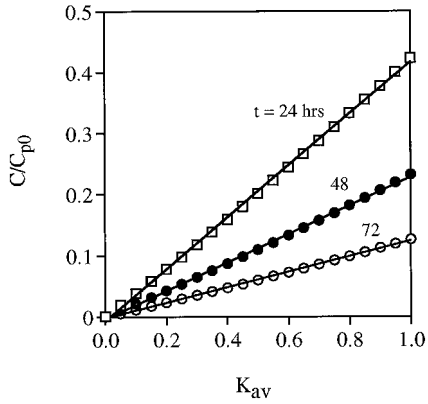

Fig. 5. Mathematical simulation of drug accumulation in a solid tumor, using Eq. F and the baseline values of constants. *Data points*, predictions of numerical simulations; *solid lines*, linear curve fittings of symbols. At 24, 48, and 72 h, the slopes of curves were 0.424, 0.232, and 0.127, respectively.

cross-link of proteoglycans by polylysine molecules reduces the available volume fraction. Another promising method for reducing tissue swelling without significantly disturbing its structures is to place tissue in a chamber with a fixed volume (9, 18). In doing so, tissue swelling effect on K_{AV} can be controlled within 10% (18). To investigate the effect of tissue swelling on the quantification of the available volume fraction, we constructed a polycarbonate chamber described in the "Materials and Methods." Tumor tissues were sectioned into 400-μm slices and cut into 4-mm discs. The discs were divided into two groups. In one group, three discs were placed in different chambers and incubated in tracer solutions. In another group, three discs were incubated freely in the same solutions. In each solution, discs were incubated for a time period longer than the equilibrium time constant. At the end of incubation, the available volume fractions of tracers were quantified and compared between two groups (Fig. 4). We found that the effect of tissue swelling on K_{AV} was less significant than that of molecular weight. There was no statistical difference between the groups (Wilcoxon signed rank test). Therefore, tumor tissues were incubated freely in most of our experiments.

Implications for Drug Delivery to Solid Tumors

Novel therapeutic agents have been developed to target specific molecules in tumor cells. These so-called molecular medicines are more specific to tumor cells in comparison with conventional drugs. However, delivery of molecular medicines to tumor cells is a critical problem because these agents are, in general, macromolecules or nanoparticles (62, 63). Transport and accumulation of macromolecules or nanoparticles in tumors are limited by various factors, including microvascular permeability (37), interstitial diffusion coefficient (32, 33), and available volume fraction. To understand how the available volume fraction affects drug accumulation in tumors, we performed a pharmacokinetic analysis, using a compartmental model. The major assumption of the model was that the tumor compartment was well mixed, *i.e.*, the concentration of drugs in the extravascular space was uniform. Thus, the governing equation is:

$$V\frac{dC}{dt} = PS(C_p - C/K_{AV}) \qquad \text{(D)}$$

where C and C_p are the concentrations in the tissue and the plasma, respectively; V is the total volume of tumor; P is the microvascular permeability; and S is the total surface area of vessels. In addition, we assumed that the transport in solid tumors would not affect significantly the plasma clearance of drugs. Therefore, the plasma concentration of macromolecules could be approximated by a biexponential function of time (28–30):

$$C_p = C_{p0}[\rho e^{-\lambda_1 t} + (1-\rho)e^{-\lambda_2 t}] \qquad \text{(E)}$$

where C_{p0} is the initial value of C_p, ρ, λ_1, and λ_2 are constants. Eqs. D and E were solved analytically to obtain the concentration of drugs in tumors:

$$\frac{C}{C_{p0}} = \lambda_3 K_{AV}\left[\frac{\rho}{\lambda_3-\lambda_1}(e^{-\lambda_1 t} - e^{-\lambda_3 t}) + \frac{1-\rho}{\lambda_3-\lambda_2}(e^{-\lambda_2 t} - e^{-\lambda_3 t})\right] \qquad \text{(F)}$$

where λ_3 ($= PS/VK_{AV}$) is the rate of drug transport from the plasma into the extravascular space of tumors. The drug accumulation in tumors, *i.e.*, the percentage of the injected dose per gram of tissue, is proportional to C/C_{p0}. The baseline values of K_{AV}, PS/V, ρ, λ_1, and λ_2 were chosen to be 0.2, 7×10^{-5} s^{-1}, 0.3, 2×10^{-4} s^{-1}, and 7×10^{-6} s^{-1}, respectively. These values were close to those used in the study of antibody transport in solid tumors (29, 30). The simulation, using Eq. F and the baseline values of constants, indicated that C/C_{p0} was nearly a linear function of K_{AV} at times longer than 24 h ($r^2 > 0.999$; Fig. 5). At 24, 48, and 72 h, the slopes of curves were 0.424, 0.232, and 0.127, respectively. However, these curves may become nonlinear if the baseline values are changed. The implication of the simulation is twofold. (*a*) Drug accumulation in tumors depends significantly on K_{AV}. Therefore, one strategy to improve drug delivery to tumors is to increase K_{AV}. (*b*) Steric molecular exclusion in tumors has to be considered in pharmacokinetic analysis of drugs. Assuming $K_{AV} = 1$ can cause a significant overestimation of drug accumulation in tumors, especially when drugs are macromolecules or nanoparticles.

ACKNOWLEDGMENTS

We thank Jennifer L. Lanzen, Jeannie M. Poulson, and Stacey A. Snyder for tumor preparations and the reviewers for helpful comments.

REFERENCES

1. Jain, R. K. Delivery of molecular and cellular medicine to solid tumors. Microcirculation, *4:* 1–23, 1997.
2. Comper, W. D., and Laurent, T. C. Physiological function of connective tissue polysaccharides. Physiol. Rev., *58:* 255–315, 1978.
3. Curry, F. E. Mechanisms and thermodynamics of transcapillary exchange. *In:* E. M. Renkin and C. C. Michel (eds.), Handbook of Physiology, Sect. 2, The Cardiovascular System, Vol. IV, The Microcirculation, pp. 309–374. Bethesda: American Physiological Society, 1984.
4. El-Kareh, A. W., Braunstein, S. L., and Secomb, T. W. Effect of cell arrangement and interstitial volume fraction on the diffusivity of monoclonal antibodies in tissue. Biophys. J., *64:* 1638–1646, 1993.
5. Granger, H. J., and Shepherd, A. P. Dynamics and control of the microcirculation. Adv. Biomed. Eng., *7:* 1–63, 1979.
6. Tong, J., and Anderson, J. L. Partitioning and diffusion of proteins and linear polymers in polyacrylamide gels. Biophys. J., *70:* 1505–1513, 1996.
7. Meyer, F. A. Macromolecular basis of globular protein exclusion and of swelling pressure in loose connective tissue (umbilical cord). Biochim. Biophys. Acta, *755:* 388–399, 1983.
8. Maroudas, A. Transport of solutes through cartilage: permeability to large molecules. J. Anat., *122:* 335–347, 1976.
9. Meyer, F. A., Koblentz, M., and Silberberg, A. Structural investigation of loose connective tissue by using a series of dextran fractions as non-interacting macromolecular probes. Biochem. J., *161:* 285–291, 1977.
10. Williams, J. C., Mark, L. A., and Eichholtz, S. Partition and permeation of dextran in polyacrylamide gel. Biophys. J., *75:* 493–502, 1998.
11. Gelman, R. A., and Silberberg, A. The effect of a strongly-interacting macromolecular probe on the swelling and exclusion properties of loose connective tissue. Connect. Tissue Res., *4:* 79–90, 1976.
12. Beckenlehner, K., Bannke, S., Spruss, T., Bernhardt, G., Schonenberg, H., and Schiess, W. Hyaluronidase enhances the activity of Adriamycin in breast cancer models *in vitro* and *in vivo*. J. Cancer Res. Clin. Oncol., *118:* 591–596, 1992.

13. Hobarth, K., Maier, U., and Marberger, M. Topical chemoprophylaxis of superficial bladder cancer with mitomycin C and adjuvant hyaluronidase. Eur. Urol., *21:* 206–210, 1992.
14. Maroudas, A. Distribution and diffusion of solutes in articular cartilage. Biophys. J., *10:* 365–379, 1970.
15. Fry, D. L. Effect of pressure and stirring on *in vitro* aortic transmural ^{125}I-albumin transport. Am. J. Physiol., *245:* H977–H991, 1983.
16. Thurn, A. L. Effects of endothelial injury on macromolecular transport in the arterial wall, Ph.D. Thesis. New York: Columbia University, 1982.
17. Wiig, H., DeCarlo, M., Sibley, L., and Renkin, E. M. Interstitial exclusion of albumin in rat tissues measured by a continuous infusion method. Am. J. Physiol., *263:* H1222–H1233, 1992.
18. Bert, J. L., Pearce, R. H., and Mathieson, J. M. Concentration of plasma albumin in its accessible space in postmortem human dermis. Microvasc. Res., *32:* 211–223, 1986.
19. Barr, L., and Malvin, R. L. Estimation of extracellular spaces of smooth muscle using different-sized molecules. Am. J. Physiol., *208:* 1042–1045, 1965.
20. Reed, R. K., and Lepsøe, S. Interstitial exclusion of albumin in rat dermis and subcutis in over- and dehydration. Am. J. Physiol., *257:* H1819–H1827, 1989.
21. Schneiderman, R., Snir, E., Popper, O., Hiss, J., Stein, H., and Maroudas, A. Insulin-like growth factor-I and its complexes in normal human articular cartilage: studies of partition and diffusion. Arch. Biochem. Biophys., *324:* 159–172, 1995.
22. Aukland, K. Distribution volumes and macromolecular mobility in rat tail tendon interstitium. Am. J. Physiol., *260:* H409–H419, 1991.
23. Karlsson, L., Alpsten, M., Appelgren, K. L., and Peterson, H-I. Intratumor distribution of vascular and extravascular spaces. Microvasc. Res., *19:* 71–79, 1980.
24. Appelgren, L., Peterson, H. I., and Rosengren, B. Vascular and extravascular spaces in two transplantable tumours of the rat. Bibl. Anat., *12:* 504–510, 1973.
25. Wist, E., Millar, J. L., and Shorthouse, A. J. Melphalan uptake in relation to vascular and extracellular space of human lung-tumour xenografts. Br. J. Cancer, *43:* 458–463, 1981.
26. Gullino, P. M., Grantham, F. H., and Smith, S. H. The interstitial water space of tumors. Cancer Res., *25:* 727–731, 1964.
27. O'Connor, S. W., and Bale, W. F. Accessibility of circulating immunoglobulin G to the extravascular compartment of solid rat tumors. Cancer Res., *44:* 3719–3723, 1984.
28. Baxter, L. T., Yuan, F., and Jain, R. K. Pharmacokinetic analysis of the perivascular distribution of bifunctional antibodies and haptens: comparison with experimental data. Cancer Res., *52:* 5838–5844, 1992.
29. Fujimori, K., Covell, D. G., Fletcher, J. E., and Weinstein, J. N. Modeling analysis of the global and microscopic distribution of immunoglobulin G, $F(ab')_2$, and Fab in tumors. Cancer Res., *49:* 5656–5663, 1989.
30. Yuan, F., Baxter, L. T., and Jain, R. K. Pharmacokinetic analysis in two-step approaches using bifunctional and enzyme-conjugated antibodies. Cancer Res., *51:* 3119–3130, 1991.
31. Shan, S. Q., Rosner, G. L., Braun, R. D., Hahn, J., Pearce, C., and Dewhirst, M. W. Effects of diethylamine/nitric oxide on blood perfusion and oxygenation in the R3230Ac mammary carcinoma. Br. J. Cancer, *76:* 429–437, 1997.
32. Berk, D. A., Yuan, F., Leunig, M., and Jain, R. K. Fluorescence photobleaching with spatial Fourier analysis: measurement of diffusion in light-scattering media. Biophys. J., *65:* 2428–2436, 1993.
33. Berk, D. A., Yuan, F., Leunig, M., and Jain, R. K. Direct *in vivo* measurement of targeted binding in a human tumor xenograft. Proc. Natl. Acad. Sci. USA, *94:* 1785–1790, 1997.
34. Gardner, C. M., Jacques, S. L., and Welch, A. J. Light transport in tissues: accurate expressions for one-dimensional fluence rate and escape function based upon Monte Carlo simulation. Lasers Surg. Med., *18:* 129–138, 1996.
35. Yuan, F., Leunig, M., Berk, D. A., and Jain, R. K. Microvascular permeability of albumin, vascular surface area and vascular volume measured in human adenocarcinoma LS174T using dorsal chamber in SCID mice. Microvasc. Res., *45:* 269–289, 1993.
36. Jain, R. K. Determinants of tumor blood flow: a review. Cancer Res., *48:* 2641–2658, 1988.
37. Yuan, F., Dellian, M., Fukumura, D., Leunig, M., Berk, D. A., Torchillin, V. P., and Jain, R. K. Vascular permeability in a human tumor xenograft: molecular size dependence and cut-off size. Cancer Res., *55:* 3752–3756, 1995.
38. Michel, C. C. Capillary permeability and how it may change. J. Physiol., *404:* 1–29, 1988.
39. Curry, F. E. Determinants of capillary permeability: a review of mechanisms based on single capillary studies in the frog. Circ. Res., *59:* 367–380, 1986.
40. Weinbaum, S., Tsay, R., and Curry, F. E. A three-dimensional junction-pore-matrix model for capillary permeability. Microvasc. Res., *44:* 85–111, 1992.
41. Weinbaum, S., Cowin, S. C., and Zeng, Y. A model for the excitation of osteocytes by mechanical loading-induced bone fluid shear stresses. J. Biomech., *27:* 339–360, 1994.
42. Fu, B. M., Weinbaum, S., Tray, R. Y., and Curry, F. E. A junction-orifice-fiber entrance layer model for capillary permeability: application to frog mesenteric capillaries. J. Biomech. Eng., *116:* 502–513, 1994.
43. Mörgelin, M., Paulsson, M., Malmström, A., and Heinegård, D. Shared and distinct structural features of interstitial proteoglycans from different bovine tissues revealed by electron microscopy. J. Biol. Chem., *264:* 12080–12090, 1989.
44. Buckwalter, J. A., and Rosenberg, L. C. Electron microscopic studies of cartilage proteoglycans. Electron Microsc. Rev., *1:* 87–112, 1988.
45. Iozzo, R. V. Proteoglycans and neoplasia. Cancer Metastasis Rev., *7:* 39–50, 1988.
46. Ogston, A. G. The spaces in a uniform random suspension of fibers. Trans. Farad Soc., *54:* 1754–1757, 1958.
47. Giddings, J. C., Kucera, E., Russell, C. P., and Myers, M. N. Statistical theory for the equilibrium distribution of rigid molecules in inert porous networks. Exclusion chromatography. J. Phys. Chem., *72:* 4397–4408, 1968.
48. Casassa, E. F. Equilibrium distribution of flexible polymer chains between a macroscopic solution phase and small voids. Polymer Lett., *5:* 773–778, 1967.
49. Johansson, L., and Löfroth, J. E. Diffusion and interaction in gels and solutions. 4. Hard sphere Brownian dynamics simulations. J. Chem. Phys., *98:* 7471–7479, 1993.
50. Phillips, R. J., Deen, W. M., and Brady, J. F. Hindered transport in fibrous membranes and gels: effect of solute size and fiber configurations. J. Colloid Interface Sci., *139:* 363–373, 1990.
51. Jain, R. K. Transport of molecules in the tumor interstitium: a review. Cancer Res., *47:* 3039–3051, 1987.
52. Dobson, G. P., and Cieslar, J. H. Intracellular, interstitial and plasma space in the rat myocardium *in vivo*. J. Mol. Cell. Cardiol., *29:* 3357–3363, 1997.
53. Yuan, F. Transvascular drug delivery in solid tumors. Semin. Radiat. Oncol., *8:* 164–175, 1998.
54. Dvorak, H. F., Nagy, J. A., Dvorak, J. T., and Dvorak, A. M. Identification and characterization of the blood vessel of solid tumors that are leaky to circulating macromolecules. Am. J. Pathol., *133:* 95–109, 1988.
55. Teraoka, I. Interferometric study of transition from weak to strong penetration of a polymer solution into a porous silica bead. Macromolecules, *29:* 2430–2439, 1996.
56. Urban, J. P. G., and Maroudas, A. Swelling of the intervertebral disc *in vitro*. Connect. Tissue Res., *9:* 1–10, 1981.
57. Canal, T., and Peppas, N. A. Correlation between mesh size and equilibrium degree of swelling of polymeric networks. J. Biomed. Material Res., *23:* 1183–1193, 1989.
58. Richerson, G. B., and Messer, C. Effect of composition of experimental solutions on neuronal survival during rat brain slicing. Exp. Neurol., *131:* 133–143, 1995.
59. Friedman, M. H., and Green, K. Swelling rate of corneal stroma. Exp. Eye Res., *12:* 239–250, 1971.
60. Buschmann, M. D., and Grodzinsky, A. J. A molecular model of proteoglycan-associated electrostatic forces in cartilage mechanics. J. Biomech. Eng., *117:* 179–192, 1995.
61. Setton, L. A., Gu, W., Lai, W. M., and Mow, V. C. Predictions of the swelling-induced pre-stress in articular cartilage. *In:* A. P. S. Selvadurai (ed.), Mechanics of Poroelastic Media, pp. 299–320. Dordrecht: Kluwer Academic Publishers, 1995.
62. Giaccia, A. J., Brown, J. M., Wouters, B., Denko, N., and Koumenis, C. Cancer therapy and tumor physiology. Science (Washington DC), *279:* 12–13, 1998.
63. Jain, R. K. The next frontier of molecular medicine: delivery of therapeutics. Nat. Med., *4:* 655–657, 1998.

Available Volume Fraction of Macromolecules in the Extravascular Space of a Fibrosarcoma: Implications for Drug Delivery

Ava Krol, Julie Maresca, Mark W. Dewhirst, et al.

Cancer Res 1999;59:4136-4141.